Kinematics of a 2-DOF Planar Suspended Cable-Driven Parallel Robot

Dinh Quan Nguyen(✉)

Le Quy Don Technical University, Hanoi, Vietnam
ndquan@lqdtu.edu.vn

Abstract. This paper discusses the kinematics of a two degrees of freedom (2-DOF) planar suspended cable-driven parallel robot (CDPR) with massless cables. The solutions for the inverse and direct geometric as well as the inverse and direct kinematic problems are derived while fully considering the influence of pulleys and cable winding drums.

Keywords: Inverse kinematics · Direct kinematics · Suspended CDPR

1 Introduction

The studies of CDPRs have been carried on for several decades. Due to their appealing advantages over rigid-body manipulators such as simple in design, having large workspace and low construction cost, there are more and more prototypes of CDPRs have been developed. However, one significant drawback of CDPRs compared to rigid-body manipulators is the low accuracy in their kinematic modeling which lead to their limits in industrial applications. Simple design CDPRs tend to bring more complexity in solving their kinematic problems, especially when all the main factors of the CDPR systems are considered, for example, pulleys and cable winding drums or the cable sag (in the case of large workspace and heavy payload CDPRs). The simpler in design, the greater difficulty there is in order to solve the kinematic modeling problem which is the well-known trade-off of CDPRs.

Over the past years, many research works have been focusing on dealing with these problems of CDPR in order to improve their performance in control applications. Basic solutions to solve the inverse and direct kinematic problems of CDPR (where the influence of pulleys and winding drums are ignored) can be seen in [1–3]. Recent studies on CDPRs that consider the involvement of pulleys can be seen in [4–6]. The works considered both the pulleys and drums of CDPR systems can be seen in [7,8], however, kinematic modeling solutions has not been developed explicitly.

Nevertheless, there is the fact that it is difficult to archive the accuracy in CDPR kinematic modeling similar to that of rigid-body manipulators. For very large dimension CDPRs, in most applications, simplified kinematic modeling solutions might be used to get satisfying results. However, for relatively small workspace CDPRs, in order to increase their applicability, it is important to

M. Gouttefarde et al. (Eds.): CableCon 2021, MMS 104, pp. 13–23, 2021.
https://doi.org/10.1007/978-3-030-75789-2_2

have a good CDPR kinematic modeling solution. We will try to find a solution regarding this problem in this paper, starting with the most basic CDPR system: a 2-DOF planar suspended CDPR with massless cables.

2 Geometric Models

Figure 1 shows the geometric structure of the 2-DOF suspended CDPR. It consists of a point mass driven by two massless cables. For this model, we have several assumptions as follows:

- The cables are massless. The cable segments that do not mount on a pulley or drum are considered as straight lines.
- The end-effector point is always lies on the plane $(\mathbf{x}_0, \mathbf{z}_0)$ of the global coordinate frame $\langle O_0 \rangle$.
- All the cables connect to the point mass at point B.
- The position of the pulleys and drums are fixed.
- The last two pulleys have the same coordinate in z-axis $(z_{P1} = z_{P2})$.
- The total lengths of the cables are the same.
- The deformations of the cable length due to friction (between pulleys or drums and cables) or due to cable twisting or ovalization are neglected.
- There is no deformation of the base frame of the CDPR system (the mounting positions of the pulleys and drums are fixed in space).
- The distance between the drums and first pulleys are large enough so that the cables lie properly in corresponding grooves of the drums.

2.1 Inverse Geometric Problem

When fully considering the influence of all the components in the cable driving system, we will find the equations where the inputs are the coordinates of point B and the output is the position of the cable exit point on the drum (or the number of cable turns on the drums).

Figure 2 describes the cable-driving system for one cable. For simplicity, the cable index $i\,(i = 1, 2)$ will be omitted in all the terms in this section. For each cable, the total cable length is constant:

$$L_T = L^{(D)} + L^{(D,E)} + L^{(E,P)} + L^{(P,B)} \tag{1}$$

where:

- L_T: total cable length.
- $L^{(D)}$: length of cable segment on the drum.
- $L^{(D,E)}$: length of cable segment from the cable exit point on the drum to the tangent point of the first pulley.
- $L^{(E,P)}$: length of cable segment from the input tangent point of the first pulley to the input tangent point of the last pulley.

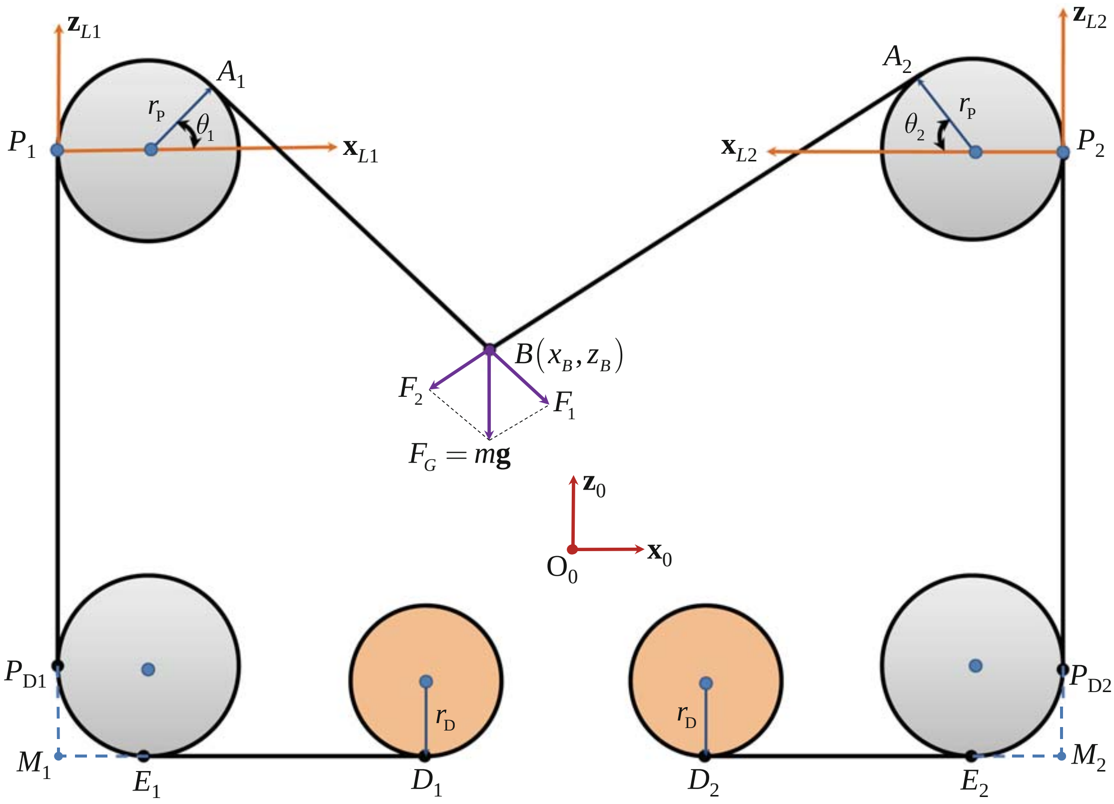

Fig. 1. Geometric structure of 2-DOF suspended CDPR.

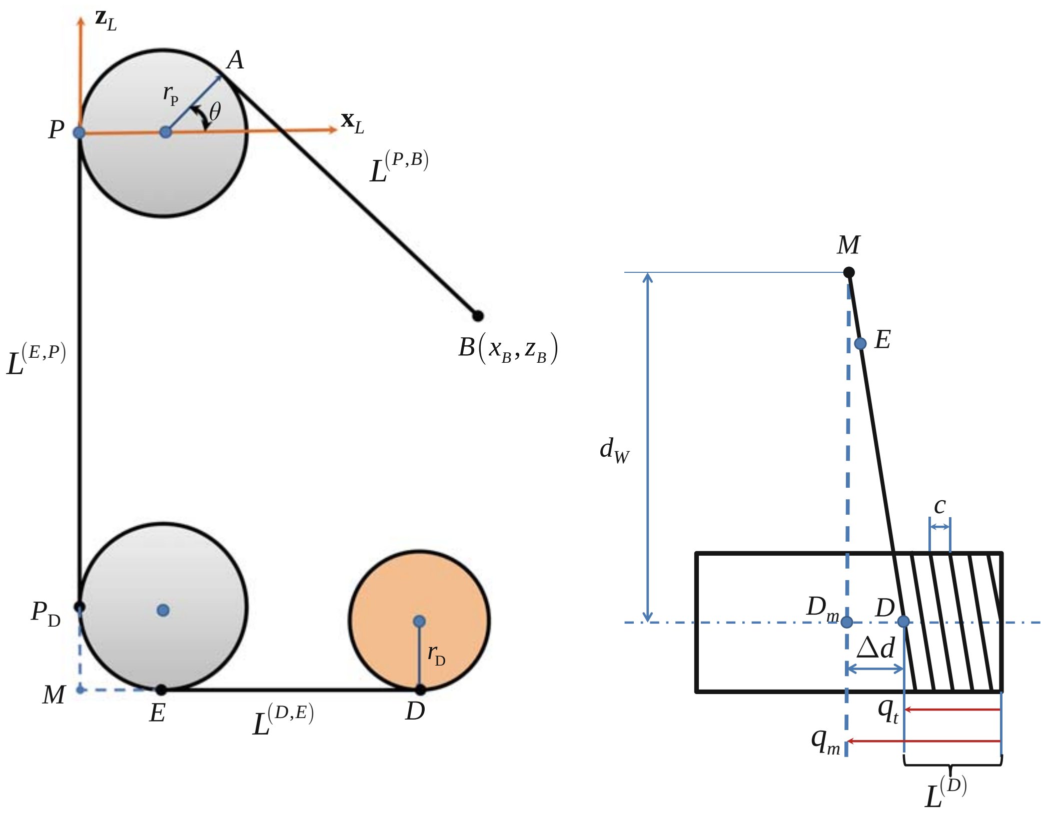

Fig. 2. Cable-driving system for one cable.

- $L^{(P,B)}$: length of cable segment from the input tangent point of the last pulley to the end-effector point.

In the following, we will compute each part of the cable. The cable segment on the drum is calculated as follows:

$$L^{(D)} = 2\pi\sqrt{r_D^2 + c^2} \cdot q_t = r_q \cdot q_t \tag{2}$$

with:

- r_D: drum radius
- c: helical step on the drum (distance between two consecutive grooves on the drum).
- q_t: current number of cable turns on the drum at time t.
- $r_q = 2\pi\sqrt{r_D^2 + c^2}$: conversion ratio between the cable length on the drum and the number of cable turns.

The cable segment from the cable exit point on the drum to the input tangent point of the first pulley:

$$\begin{aligned} L^{(D,E)} &= MD - ME \\ &= \sqrt{d_w^2 + \triangle d^2} - r_p \\ &= \sqrt{d_w^2 + c^2\left(q_t - q_m\right)^2} - r_p \end{aligned} \tag{3}$$

with:

- d_w: distance from M to the orthogonal cable exit point D_m on the drum (Fig. 2).
- $\triangle d = c \cdot \triangle q$: distance from the cable exit point D to the orthogonal cable exit point D_m on the drum.
- r_P: pulley radius.
- $\triangle q = (q_t - q_m)$: difference in cable turns from the point D_m to D.
- q_m: number of cable turns on the drum with respect to the cable exit point at D_m.

The cable segment from the input tangent point of the first pulley to the input tangent point of the last pulley:

$$L^{(E,P)} = L^{(P_D,P)} + \frac{\pi}{2} r_P \tag{4}$$

The term $L^{(P_D,P)}$ is determined since all the pulleys are fixed at the pivot points (P_D, P).

The cable segment from the input tangent point of the last pulley to the end-effector point:

$$L^{(P,B)} = L_t + (\pi - \theta_t)\, r_P \tag{5}$$

The term L_t is calculated as follows:

$$L_t = \|AB\| = \sqrt{\left(x_B - x_A\right)^2 + \left(z_B - z_A\right)^2} \tag{6}$$

In Eq. (6), the coordinates of point A need to be computed through the tangent equation of the line AB to the pulley inner circle, expressed in the local cable coordinate frame at point P. The subscript "L" is used to indicate that all the terms are expressed in the cable local coordinate frame $\langle P \rangle$. The coordinates of point B in frame $\langle P \rangle$ are:

$$\begin{aligned} x_{LB} &= |x_B - x_P| \\ z_{LB} &= z_B - z_P \end{aligned} \tag{7}$$

The coordinates of point A in the frame $\langle P \rangle$ are computed as follows:

$$\begin{aligned} z_{LA} &= \frac{z_{LB} r_P^2 + r_P \left| x_{LB} - r_P \right| \sqrt{z_{LB}^2 + \left(x_{LB} - r_P\right)^2 - r_P^2}}{z_{LB}^2 + \left(x_{LB} - r_P\right)^2} \\ x_{LA} &= r_P + \sqrt{r_P^2 - z_{LA}^2} \end{aligned} \tag{8}$$

The coordinates of point A in the global coordinate frame $\langle O_0 \rangle$ are:

$$\begin{aligned} x_A &= x_P + x_{LA} \cos\left(\gamma\right) \\ z_A &= z_P + z_{LA} \end{aligned} \tag{9}$$

with the angle γ is computed as follows:

$$\gamma = \operatorname{atan2}\left(0, x_B - x_P\right) \tag{10}$$

To determine the term q_t, let us rewrite the Eq. (1) after substituting all the calculated terms:

$$L_T = r_q q_t + \sqrt{d_w^2 + c^2 \left(q_t - q_m\right)^2} + L^{(P_D,P)} + L_t + \left(\frac{3\pi}{2} - \theta_t - 1\right) r_P \tag{11}$$

In Eq. (11), we have:

- L_t is determined from Eqs. (6)–(10).
- θ_t can be computed from Eq. (7):

$$\theta_t = \operatorname{asin}\left(\frac{z_{LA}}{r_P}\right) \tag{12}$$

- q_m is determined from the CDPR design.

Deriving Eq. (11), we get:

$$\sqrt{d_w^2 + c^2 \left(q_t - q_m\right)^2} = M - r_q q_t \tag{13}$$

where:

$$M = L_T - L^{(P_D,P)} - L_t - \left(\frac{3\pi}{2} - \theta_t - 1\right) r_P \tag{14}$$

Equation (13) has two roots:

$$q_t = \frac{-\left(c^2 q_m - r_q M\right) \pm \sqrt{\triangle}}{r_q^2 - c^2} \tag{15}$$

with:

$$\triangle = \left(r_q^2 - c^2\right) d_w^2 + c^2 \left(r_q q_m - M\right)^2 \tag{16}$$

Note that q_t always has positive value. Besides, from Eq. (13) we have:

$$M - r_q q_t > 0 \tag{17}$$

If we choose $q_t = \frac{-\left(c^2 q_m - r_q M\right) + \sqrt{\triangle}}{r_q^2 - c^2}$, substituting this solution in condition (17) we have:

$$M - r_q \frac{-\left(c^2 q_m - r_q M\right) + \sqrt{\triangle}}{r_q^2 - c^2} = \frac{-c^2 \left(M - r_q q_m\right) - \sqrt{\triangle}}{r_q^2 - c^2} > 0 \tag{18}$$

which is not valid. Therefore, Eq. (13) has only one root:

$$q_t = \frac{-\left(c^2 q_m - r_q M\right) - \sqrt{\triangle}}{r_q^2 - c^2} \tag{19}$$

Equation (19) is the solution of the inverse geometric problem: given the coordinates of the end-effector point, find the number of cable turns on the drum.

Also, from Eq. (19) one can see that, in order to calculate exactly the value of q_t, we need to know exactly the values of the following terms: q_m, d_w, L_T and the coordinates of each pulley (in this study case are the coordinates of points P and P_D). The determination of these terms depends on the accuracy of machining and assembling all the parts of the CDPR.

2.2 Direct Geometric Problem

For the CDPR in this work, we will derive the constraint equations that describe the relations between the coordinates of the end-effector point and the number of cable turns on each drum q_{ti} $(i = 1, 2)$.

Derive Eq. (11) for two cables, we have:

$$L_i + \theta_i r_P = L_{ti} \qquad (i = 1, 2) \tag{20}$$

with:

$$L_i = L_{Ti} - r_q q_{ti} - \sqrt{d_{wi}^2 + c^2 \left(q_{ti} - q_{mi}\right)^2} - L^{(P_{Di}, P_i)} - \left(\frac{3\pi}{2} - 1\right) r_P \qquad (i = 1, 2) \tag{21}$$

Therefore, if $q_{ti}\,(i=1,2)$ are known, one can compute $L_i\,(i=1,2)$. From Eq. (20), we have:

$$(L_i+\theta_i r_P)^2=(x_{LAi}-x_{LBi})^2+(z_{LAi}-z_{LBi})^2 \qquad (i=1,2) \tag{22}$$

All the coordinates in Eq. (22) are expressed in the local cable coordinate frames that have their origins at the mounting points of respective pulleys, and are computed as follows $(i=1,2)$:

$$\begin{cases} x_{LAi}=r_P\,(C_i+1)\\ z_{LAi}=r_P S_i\\ x_{LBi}=|x_B-x_{Pi}|\\ z_{LBi}=z_B-z_{Pi} \end{cases} \tag{23}$$

with $C_i=\cos(\theta_i)\,,S_i=\sin(\theta_i)\quad(i=1,2)$. All the terms that have the subscripts "L" and "i" are expressed in the local cable coordinate frames that have their origins at P_i. All the terms without the subscript "L" are expressed in the global coordinate frame $\langle O_0\rangle$. The tangent equations of the line BA_i expressed in the local cable coordinate frames:

$$(x_{LAi}-r_P)\,(x_{LBi}-r_P)+z_{LAi}z_{LBi}=r_P^2 \qquad (i=1,2) \tag{24}$$

which leads to:

$$\begin{gathered} r_P C_i\,(x_{LBi}-r_P)+r_P S_i z_{LBi}=r_P^2\\ \Rightarrow\begin{cases} z_{LBi}=\dfrac{r_P-C_i\,(x_{LBi}-r_P)}{S_i}\\ x_{LBi}=\dfrac{r_P-S_i z_{LBi}}{C_i}+r_P \end{cases} \qquad (i=1,2) \end{gathered} \tag{25}$$

Note that the angles $\theta_i\ \ (i=1,2)$ are strictly constrained by the following condition:

$$0<\theta_i<\frac{\pi}{2} \qquad (i=1,2) \tag{26}$$

Therefore, $S_i>0,\ C_i>0\ \ (i=1,2)$, thus $z_{LBi},\ x_{LBi}$ are always exist. The condition (26) only happens when the end-effector point lies within the feasible workspace which satisfies the conditions of the tension distribution problem where the end-effector is at its static equilibrium. In the cases the end-effector moves, there could be situations where the angles θ_i fall outside the range in (26) but the cable tensions are still positive. These cases are not considered in this study.

Substituting Eqs. (23), (25) into Eq. (22), we have:

$$(L_i+\theta_i r_P)^2=\frac{1}{C_i^2}\,(z_{LAi}-z_{LBi})^2 \qquad (i=1,2) \tag{27}$$

For suspended CDPR, we have the condition:

$$z_{LAi}>z_{LBi} \qquad (i=1,2) \tag{28}$$

Thus, Eq. (27) becomes:

$$\begin{aligned} L_i + \theta_i r_P &= \frac{1}{C_i}\left(z_{LAi} - z_{LBi}\right) \\ \Leftrightarrow z_{LBi} &= r_P S_i - C_i\left(L_i + \theta_i r_P\right) \qquad (i = 1, 2) \end{aligned} \tag{29}$$

From Eq. (23) and Eq. (29) we have:

$$z_B = z_{Pi} + r_P S_i - C_i\left(L_i + \theta_i r_P\right) \qquad (i = 1, 2) \tag{30}$$

Substituting Eq. (29) into Eq. (25) we have:

$$\begin{aligned} x_{LBi} &= \frac{r_P - S_i\left[r_P S_i - C_i\left(L_i + \theta_i r_P\right)\right]}{C_i} + r_P \\ \Rightarrow x_{LBi} &= r_P\left(C_i + 1\right) + S_i\left(L_i + \theta_i r_P\right) \qquad (i = 1, 2) \end{aligned} \tag{31}$$

From Eq. (23) and Eq. (31) we have:

$$\left|x_B - x_{Pi}\right| = r_P\left(C_i + 1\right) + S_i\left(L_i + \theta_i r_P\right) \qquad (i = 1, 2) \tag{32}$$

Combining Eq. (30) and Eq. (32) and note the condition $x_{P1} < x_B < x_{P2}$, we have a system of four equations with four unknown terms $(x_B, z_B, \theta_1, \theta_2)$:

$$\begin{cases} x_B = x_{P1} + r_P\left(C_1 + 1\right) + S_1\left(L_1 + \theta_1 r_P\right) \\ x_B = x_{P2} - r_P\left(C_2 + 1\right) - S_2\left(L_2 + \theta_2 r_P\right) \\ z_B = z_{P1} + r_P S_1 - C_1\left(L_1 + \theta_1 r_P\right) \\ z_B = z_{P2} + r_P S_2 - C_2\left(L_2 + \theta_2 r_P\right) \end{cases} \tag{33}$$

The system of equations (33) does not have analytical solution. That is why we have to use numerical methods to compute the unknown terms $(x_B, z_B, \theta_1, \theta_2)$ in which (x_B, z_B) is the solution of the direct geometric problem.

Derive the Eq. (33) and note that $z_{P1} = z_{P2}$, we can transform the system of equations to:

$$\begin{cases} S_{12}\left(L_1 + r_P\theta_1\right) - \left(x_{P2} - x_{P1} - 2r_P\right)C_2 + r_P\left(C_{12} + 1\right) = 0 \\ S_{12}\left(L_2 + r_P\theta_2\right) - \left(x_{P2} - x_{P1} - 2r_P\right)C_1 + r_P\left(C_{12} + 1\right) = 0 \\ x_B = x_{P1} + r_P\left(C_1 + 1\right) + S_1\left(L_1 + \theta_1 r_P\right) \\ z_B = z_{P1} + r_P S_1 - C_1\left(L_1 + \theta_1 r_P\right) \end{cases} \tag{34}$$

where $S_{12} = \sin\left(\theta_1 + \theta_2\right), C_{12} = \cos\left(\theta_1 + \theta_2\right)$.

Equation (34) can be solved through two steps as follows.

Step 1: *Using numerical methods to compute* θ_1, θ_2 from the first two equations:

$$\begin{cases} f_1\left(\boldsymbol{\theta}\right) = S_{12}\left(L_1 + r_P\theta_1\right) - \left(x_{P2} - x_{P1} - 2r_P\right)C_2 + r_P\left(C_{12} + 1\right) = 0 \\ f_2\left(\boldsymbol{\theta}\right) = S_{12}\left(L_2 + r_P\theta_2\right) - \left(x_{P2} - x_{P1} - 2r_P\right)C_1 + r_P\left(C_{12} + 1\right) = 0 \end{cases} \tag{35}$$

with $\boldsymbol{\theta} = \left[\theta_1 \quad \theta_2\right]^T$.

Let us define $\mathbf{F}(\boldsymbol{\theta}) = [f_1(\boldsymbol{\theta}) \quad f_2(\boldsymbol{\theta})]^T$. Using the Newton-Raphson method, the solution of (35) is updated as follows:

$$\begin{aligned} \boldsymbol{\theta}^{(k)} &= \boldsymbol{\theta}^{(k-1)} + \triangle\boldsymbol{\theta}^{(k-1)} \\ \triangle\boldsymbol{\theta}^{(k-1)} &= -\mathbf{J}_a\left(\boldsymbol{\theta}^{(k-1)}\right)^{-1}\mathbf{F}\left(\boldsymbol{\theta}^{(k-1)}\right) \end{aligned} \tag{36}$$

with:

$$\begin{aligned} \mathbf{J}_a(\boldsymbol{\theta}) &= \begin{bmatrix} \frac{\partial f_1}{\partial \theta_1} & \frac{\partial f_1}{\partial \theta_2} \\ \frac{\partial f_2}{\partial \theta_1} & \frac{\partial f_2}{\partial \theta_2} \end{bmatrix} \\ \frac{\partial f_1}{\partial \theta_1} &= C_{12}(L_1 + r_P\theta_1) \\ \frac{\partial f_1}{\partial \theta_2} &= C_{12}(L_1 + r_P\theta_1) + (x_{P2} - x_{P1} - 2r_P)S_2 - r_P S_{12} \\ \frac{\partial f_2}{\partial \theta_1} &= C_{12}(L_2 + r_P\theta_2) + (x_{P2} - x_{P1} - 2r_P)S_1 - r_P S_{12} \\ \frac{\partial f_2}{\partial \theta_2} &= C_{12}(L_2 + r_P\theta_2) \end{aligned} \tag{37}$$

For a general case, one can start with the initial condition:

$$\begin{aligned} \boldsymbol{\theta}^{(0)} &= [\pi/4 \quad \pi/4]^T \\ \triangle\boldsymbol{\theta}^{(0)} &= -\mathbf{J}_a\left(\boldsymbol{\theta}^{(0)}\right)^{-1}\mathbf{F}\left(\boldsymbol{\theta}^{(0)}\right) \end{aligned} \tag{38}$$

We reach a solution when $\|\triangle\boldsymbol{\theta}\| \to 0$.

In the trajectory tracking control problem, where we have to continuously update $\boldsymbol{\theta} = \boldsymbol{\theta}_t$, the initial value $\boldsymbol{\theta}_t^{(0)}$ can be chosen as its previous values: $\boldsymbol{\theta}_t^{(0)} = \boldsymbol{\theta}_{t-1}$.

Step 2: *Update the coordinates of the end-effector point* by the last two equations in Eq. (34).

3 Kinematic Models

The kinematic models of the robot describe the relation between the velocity vector of the end-effector point B with respect to the angular velocity of the drums in term of $\dot{q}_{t1}, \dot{q}_{t2}$. In order to derive the kinematic equations, we will consider Eqs. (21), (33).

Taking the time derivatives of both sides of Eq. (21), we have:

$$\dot{L}_i = r_i \dot{q}_{ti} \qquad (i = 1, 2) \tag{39}$$

with:

$$r_i = -\left[r_q + \frac{c^2(q_{ti} - q_{mi})}{\sqrt{d_{wi}^2 + c^2(q_{ti} - q_{mi})^2}}\right] \qquad (i = 1, 2) \tag{40}$$

Taking the time derivatives of both sides of equations in Eq. (33), we have:

$$\begin{cases} \dot{x}_B = r_1 S_1 \dot{q}_{t1} + C_1 \left(L_1 + r_P \theta_1\right) \dot{\theta}_1 \\ \dot{x}_B = -r_2 S_2 \dot{q}_{t2} - C_2 \left(L_2 + r_P \theta_2\right) \dot{\theta}_2 \\ \dot{z}_B = -r_1 C_1 \dot{q}_{t1} + S_1 \left(L_1 + r_P \theta_1\right) \dot{\theta}_1 \\ \dot{z}_B = -r_2 C_2 \dot{q}_{t2} + S_2 \left(L_2 + r_P \theta_2\right) \dot{\theta}_2 \end{cases} \tag{41}$$

Rewrite Eq. (41) in the matrix form:

$$\begin{bmatrix} \dot{x}_B \\ \dot{x}_B \\ \dot{z}_B \\ \dot{z}_B \end{bmatrix} = \begin{bmatrix} C_1 \left(L_1 + r_P \theta_1\right) & 0 & r_1 S_1 & 0 \\ 0 & -C_2 \left(L_2 + r_P \theta_2\right) & 0 & -r_2 S_2 \\ S_1 \left(L_1 + r_P \theta_1\right) & 0 & -r_1 C_1 & 0 \\ 0 & S_2 \left(L_2 + r_P \theta_2\right) & 0 & -r_2 C_2 \end{bmatrix} \cdot \begin{bmatrix} \dot{\theta}_1 \\ \dot{\theta}_2 \\ \dot{q}_{t1} \\ \dot{q}_{t2} \end{bmatrix} \tag{42}$$

The solution for Eq. (42) is:

$$\begin{cases} \dot{\theta}_1 = \dfrac{1}{L_1 + r_P \theta_1} \left(C_1 \dot{x}_B + S_1 \dot{z}_B\right) \\ \dot{\theta}_2 = \dfrac{1}{L_2 + r_P \theta_2} \left(C_2 \dot{x}_B - S_2 \dot{z}_B\right) \\ \dot{q}_{t1} = \dfrac{1}{r_1} \left(S_1 \dot{x}_B - C_1 \dot{z}_B\right) \\ \dot{q}_{t2} = \dfrac{1}{r_2} \left(S_2 \dot{x}_B + C_2 \dot{z}_B\right) \end{cases} \tag{43}$$

From the last two equations in Eq. (43), we get the direct and inverse kinematic equations of the CDPR:

$$\begin{matrix} \dot{\mathbf{X}} = \mathbf{J} \dot{\mathbf{q}} \\ \dot{\mathbf{q}} = \mathbf{J}^{-1} \dot{\mathbf{X}} \end{matrix} \tag{44}$$

where $\mathbf{X} = \left[x_B, z_B\right]^T, \dot{\mathbf{X}} = \left[\dot{x}_B, \dot{z}_B\right]^T, \mathbf{q} = \left[q_{t1}, q_{t2}\right]^T, \dot{\mathbf{q}} = \left[\dot{q}_{t1}, \dot{q}_{t2}\right]^T$ (with unit in *rps - round per second*) and $\mathbf{J}, \mathbf{J}^{-1}$ are the Jacobian matrix and its inverse:

$$\mathbf{J} = \frac{1}{S_{12}} \begin{bmatrix} r_1 C_2 & -r_2 C_1 \\ -r_1 S_2 & -r_2 S_1 \end{bmatrix}, \qquad \mathbf{J}^{-1} = \begin{bmatrix} \dfrac{S_1}{r_1} & -\dfrac{C_1}{r_1} \\ -\dfrac{S_2}{r_2} & -\dfrac{C_2}{r_2} \end{bmatrix} \tag{45}$$

Note that we have $r_i > 0 \, (i = 1, 2)$ and $S_{12} > 0 \left(\text{because } \; 0 < \theta_1, \theta_2 < \dfrac{\pi}{2}\right)$, thus there is no singularity in the CDPR feasible work space.

4 Conclusion

This paper presented a solution in solving the direct and inverse geometric and kinematic problems of a 2-DOF planar suspended CDPR. Analytical solution can be found for the inverse geometric problem whereas only numerical solution can be found for the direct geometric problem of the CDPR.

The found solutions help to improve the accuracy of the CDPR kinematic modeling since the influence of the pulleys and cable winding drums are both considered. These results can be used in the kinematic analysis as well as in the kinematic-based control of CDPRs with a similar structure to the one in this work.

References

1. Merlet, J.-P.: The kinematics of redundant N-1 wire driven parallel robot. In: IEEE International Conference on Robotics and Automation, USA (2012)
2. Abbasnejad, G., Carricato, M.: Direct geometrico-static problem of underconstrained cable-driven parallel robots with n cables. IEEE Trans. Robot. **31**, 468–478 (2015)
3. Pott, A., Schmidt, V.: On the forward kinematics of cable-driven parallel robots. In: IEEE International Conference on Intelligent Robots and Systems, pp. 928–934 (2015)
4. Paty, T., Binaud, N., Caro, S., Segonds, S.: Cable-driven parallel robot modelling considering pulley kinematics and cable elasticity. Mech. Mach. Theory **159**(5), 104263 (2021)
5. Santos, J.C., Gouttefarde, M.: A real-time capable forward kinematics algorithm for cable-driven parallel robots considering pulley kinematics. In: Advances in Robot Kinematics 2020, Slovenia (2020)
6. Jin, X., Jung, J., Piao, J., Choi, E., Park, J.-O., Kim, C.-S.: Solving the pulley inclusion problem for a cable-driven parallel robotic system: Extended kinematics and twin-pulley mechanism. J. Mech. Sci. Technol. **32**(6), 2829–2838 (2018)
7. Schmidt, V.L.: Modelling techniques and reliable real-time implementation of kinematics for cable-driven parallel robots using polymer fiber cables. Ph.D. thesis, Fraunhofer Verlag, Stuttgart (2017)
8. Mousavi, M.R., Ghanbari, M., Moosavian, S.A.A., et al.: Explicit dynamics of redundant parallel cable robots. Nonlinear Dyn. **94**, 2077–2096 (2018)